good case for developing new numerical algorithms which take advantage of these properties.

We develop two new algorithms for computing solutions of partial differential equations, namely the adaptive application of operators to functions and the adaptive pointwise product of functions. These algorithms are necessary ingredients of any fast, adaptive numerical scheme for computing solutions of partial differential equations. The algorithm for adaptively multiplying operators and functions is based on a vanishing-moment property associated with the nonstandard form representation of a class of operators, which includes differential operators and Hilbert

$$u_t = Lu + Nf(u) \tag{2.1}$$

with the initial condition

$$u(x, 0) = u_0(x), \quad 0 \le x \le 1, \tag{2.2}$$

and the periodic boundary condition

$$u(0, t) = u(1, t), \quad 0 \le t \le T. \tag{2.3}$$

We explicitly separate the evolution Eq. (2.1) into a linear part, $Lu$, and a nonlinear part, $Nf($

$$\mathbf{Lu} = \nu \nabla^2 \mathbf{u} \tag{2.11}$$

and

$$\mathbf{Nu} = -\frac{1}{2}\left[\mathbf{u} \cdot \nabla \mathbf{u} + \nabla (\mathbf{u} \cdot \mathbf{u})\right] - \nabla (D^{-1} f(\mathbf{u})). \tag{2.12}$$

The term $D^{-1} f(\mathbf{u})$ is an integral operator which introduces a long-range interaction and has a sparse representation in wavelet bases. A one-dimensional model that may be disadvantage in that the linear and nonlinear contributions must be added in the same domain, either the physical space or the Fourier space. For solutions which exhibit shock-like solutions such transformations between the domains is costly, whereas the transform into the wavelet domain is much less expensive due to the locality of the wavelet transform. This difficulty becomes significant when one attempts to compute solutions of differential equations in multiple dimensions. We note that our wavelet approach

nonlinearity we seek approximations to integrals of the form

$$I(t) = \int_{t_0}^{t} e^{(t-\tau)L} u(\tau) v(\tau)\, d\tau, \tag{2.16}$$

where we have suppressed the explicit $x$-dependence of $u(x, t)$. In order to derive an approximation to this integral, we partition the interval of integration $[t_0, t]$ into $m$ equal subintervals with grid pointf111t0.00inter9 ◊14 1 Tfderi2054 Tm(pe(tg)-2101 0233 676.6 0 0 9ŁƒŁ833965 2v)artndƒ8 u33

For $m = 1$, we approximate (2.19) by

$$I(t) = \tfrac{1}{2} O_{L,1}(u(t_0)u_x(t_0) + u(t_1)u_x(t_1)) + O((\Delta t)^2), \tag{2.20}$$

or

$$I(t) = \tfrac{1}{2} O_{L,1}(u(t_0)u_x(t_1) + u(t_1)u_x(t_0)) + O((\Delta t)^2), \tag{2.21}$$

where

As usual, we define an associated sequence of subspaces $\mathbf{W}_j$ as the orthogonal complements of $\mathbf{V}_j$ in $\mathbf{V}$

$J \# n$. Once again we refer the reader to Appendix A and [18, 30, 33] for additional introductory and background ma-

$a_l^j$

LEMMA 1. *If the wavelet basis has M vanishing moments, then the B-blocks of the NS-form of the analytic operator function $f(\cdot_x)$, described in Section 3.2, satisfy*

$$\sum_{l \geq y} l^m b_l^j = 0 \tag{3.25}$$

*for $m = 0, 1, 2, \ldots, M-1$ and $j = 1, 2, \ldots, J$.*

*Proof.* See Appendix A.3.

LEMMA 2. *Under the conditions of Lemma 1, the B-blocks of the NS-form of the Hilbert transform*

$$(Hf)(x) = \frac{1}{\pi}\,\text{p.v.} \int_{-\infty}^{\infty} \frac{f(s)}{x - s}\, ds$$

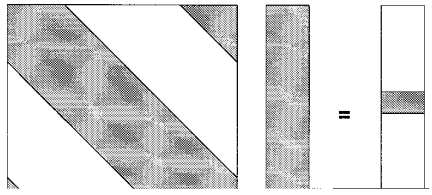

**FIG. 1.** For the operators considered in Section 3.3 the vanishing-moment property of the rows of the *B*-block yields a sparse result (up to a given accuracy «) when applied to a smooth and dense vector $\{s^j\}$.

whereas for the error we have

$$\|(P_0 f)_\epsilon(x) - (P_0 f)(x)\|_2 = \left( \sum_{j=1}^{J} \sum_{k:|d_k^j|<\epsilon} |d_k^j|^2 \right)^{1/2}, \quad \epsilon N_r^{1/2}, \tag{3.34}$$

where $N_r$ is the number of coefficients below the threshold. The number of significant wavelet coefficients is defined as $N_s = N - N_r$, where $N$ is the dimension of the space $\mathbf{V}_0$.

We define the $\epsilon$-**accurate subspace for** $f$, denoted $\mathbf{D}_f^\epsilon$, $\mathbf{V}_0$, as the subspace spanned by only those basis functions present in (3.33),

$$\mathbf{D}_f^\epsilon = \mathbf{V}_J < \text{span}\{c_{j,k}(x)\}$$

If $u(x)$ is expanded in a basis,

$$u(x) = \sum_{i=1}^{N} u_i b_i(x), \tag{4.1}$$

where $u_i$ are the coefficients and $b_i(x)$ are the basis functions, then in general

$$f(u(x)) \neq \sum_{i=1}^{N} f(u_i) b_i(x). \tag{4.2}$$

Clearly, this is the case for Fourier expansions.

Let us now assume that $u$ and $f(u)$ are *both* elements of $\mathbf{V}_0$. Then

$$u^2 = \sum_{j \in \mathbb{Z}} 2(P_j u)(Q_j u) + (Q_j u)^2, \tag{4.8}$$

which is essentially the paraproduct; see [27].

Evaluating (4.7) requires computing $(Q_j u)^2$ and $(P_j u)(Q_j u)$, where $Q_j u$ and $P_j u$ are elements of subspaces on the same scale and, thus, have basis functions with the same size support. In addition, we need to compute $(P_j u)^2$ which involves only the coarsest scale and is not computationally expensive. The difficulty in evaluating (4.7) is that the terms $(Q_j u)^2$ and $(P_j u)$ do not necessarily belong to

We then project the representation on subspaces $\mathbf{V}_{j_2 j_0}$, for $j = j_f, ..., J$ into the wavelet basis. This procedure is completely equivalent to the decomposition one has to perform after applying the NS-form. The algorithm for computing the projection of $u^2$ in a wavelet basis is illustrated in Fig. 2. In analogy with ''pseudo-spectral'' schemes, as in, e.g., [34, 35], we refer to this as an *adaptive pseudo-wavelet algorithm*.

To demonstrate that the algorithm is adaptive, we recall that $u$ has a sparse representation in the wavelet basis. Thus, evaluating $(Q_j u)^2$ for $j = 1, 2, ..., J$ requires manipulating only sparse vectors. Evaluating the square of the final coarse scale averages $(P_J u)^2$ is inexpensive. The difficulty in evaluating (4.10) lies in evaluating the products $\mathbf{R}^j_{j_0}(P_j u)(\mathbf{R}^j_{j_0} Q_j u)$ since the vectors $P_j u$ are typically dense. The adaptivity of the algorithm comes from an observation that, in the products appearing in (4.10), we may use the coefficients $Q_j u$ as a ''mask'' of the $P_j u$ (this is similar to the algorithm for adaptively applying operators to functions). In this way contributions to (4.10) are calculated, based on the presence of significant wavelet coefficients $Q_j$

rapidly converging Taylor series expansions, e.g., $f(u) = \sin(u)$ for $\|u\|$ sufficiently small. In this case, for a given accuracy $\varepsilon$ we fix an $N$ so that $\|E_{j,N}(f, u)\| < \varepsilon$. We note that the partial differential Eq. (2.1) typically involves functions $f(?)$ that are not only analytic but in many cases are $p$-degree polynomials in $u$. If this is the case then for each fixed $j$ the series in (4.13) is of degree $p$ and $E_{j,N}(f, u) = 0$ for $N > p$. In any event we are led to evaluate the double sum in (4.14), which can be done using the adaptive pseudo-wavelet algorithm described in Section 4.1.

If the function $f$ is not analytic, e.g., $f(u) = \|u\|$, then the primary concern is how to quantify an appropriate value of $j_0$, i.e., how fine a reconstruction (or how much ''oversampling'') is needed to take advantage of the interpolating property $s_0^k = u(k)$. On the other hand, determining $j_0$ may become a significant problem even if $f$ is analytic. For example if the Taylor series expansion of $f(u)$ does not converge rapidly, as in the case of $f(u) = e^u$ for large $u$, we have to consider alternate approaches.

For example, expanding $e^u$ in the ''telescopic'' series

cients. Equation (5.10) can be viewed as a simple representative of this class of equations and we emphasize that the following remarks are applicable to the variable coefficient case, $n = n(x)$ (see also [41]).

For diffusion-type equations, explicit finite difference schemes are conditionally stable with the stability condition $n\,\Delta t/(\Delta x)^2 \le 1$ (see, e.g., [2, 3]), where $\Delta t = 1/N_t$, $\Delta x = 1/N$, and $N_t$ is the number of time steps. This condition tends to require prohibitively small time steps. An alternate, implicit approach is the Crank–Nicholson scheme [2, 3], which is unconditionally stable and accurate to $O((\Delta t)^2 + (\Delta x)^2)$. At each time step, the Crank–Nicholson scheme requires solving a system of equations,

$$AU(t_{j+1}) = BU(t_j) \tag{5.12}$$

for $j = 0, 1, 2, \ldots, N_t - 1$, where we have suppressed the dependence of $U(x, t)$ on $x$. The matrices $A$ and $B$ are

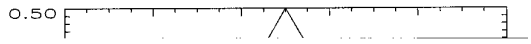


**FIG. 3.** Solution of the heat equation using the Crank–Nicholson method (5.12) with $\Delta t = \Delta x = 2^{29}$ and $n = 1.0$. Note the slowly decaying peak in the solution that is due to the eigenvalue $l_N = -0.99902344$.

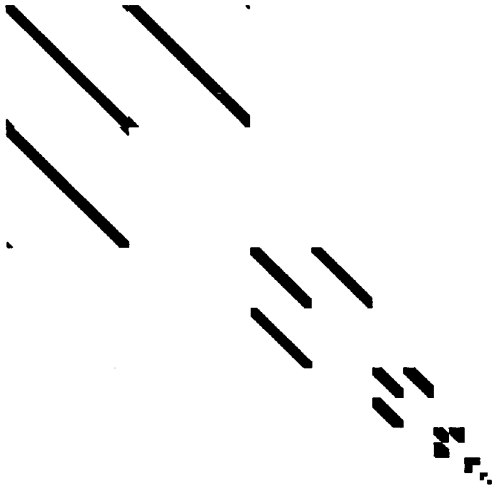

**FIG. 5.** NS-form representation of the operator $A^{21}B$ used in the

Let us conclude by reiterating that the wavelet based scheme via (5.13) is explicit and unconditionally stable. The accuracy in the spatial variable of our scheme is $O((\Delta x)^{2M})$, where $M$ is the number of vanishing moments, $\Delta x = 2^{2n}$, and $n$ is the number of scales in the multiresolution analysis. Additionally, our scheme is spectrally accurate in time. Also it is adaptive simply by virtue of using a sparse data structure to represent the operator $e^{n\Delta t \cdot_{xx}}$, the adaptive algorithm developed in Section 3.4 and the sparsity of the solution in the wavelet basis. Finally, we note that if we were to consider (5.10) with variable coefficients, e.g.,

$$u_t = n(x)u_{xx}, \tag{5.16}$$

the exponential operator $e^{\Delta t n(x) L}$ can be computed in $O(N)$ operations using the scaling and squaring method outlined in, e.g., [26] (see also [43]).

tic involved in a numerical scheme leads to a loss of accuracy in directly calculating $u(x, t)$ via (5.19), most notably within the vicinity of the shock.

Our numerical scheme for computing approximations to the solution of (5.17) consists of evaluating

$$U(t_{i+1}) = e^{\Delta t L} U(t_i) + \sum_{l=1}^{m} \alpha_{L,l} [U(t_i) - {}_x U(t_{i+1}) + U(t_{i+1}) - {}_x U(t_i)], \tag{5.21}$$

subject to the stopping criterion (5.7). Since the solution is expressed as the sum (5.21) and the linear part is equivalent, increases during the formation of the shock, yet it never exceeded 10 over the entire simulation. The compression ratios of the NS-form representation of the first derivative, exponential, and nonlinear operator $\alpha_{L,m}$ are 442.2, 3708.5, and 1364.9, respectively, where the compression ratio is defined as $N^2/N_s$, where $N$ is the dimension of the finest subspace $\mathbf{V}_0$ and $N_s$ is the number of significant entries.

EXAMPLE 2. In this example we illustrate the wavelet analogue of the Gibbs phenomena encountered when one does not use a sufficiently resolved basis expansion of the solution. In this example $n = 10$, $J = 4$, $\Delta t = 0.001$, $n = 0.001$, and $\varepsilon = 10^{-6}$, and we refer to Figs. 9 and 10. Using

**FIG. 7.** The projection on $\mathbf{V}_0$ of the solution of Burgers' equation at various time steps computed via the iteration (5.21). In this experiment $n = 15$, $J = 9$, $\Delta t = 0.001$, $\nu = 0.001$, and $\varepsilon = 10^{-6}$. This figure corresponds to Example 1 of the text.

EXAMPLE 4. In this example we set $b = a = 1$ and $l = -1$, and consider the evolution of a gaussian initial condition centered on the interval $0 \le x \le 1$, e.g., $u(x, 0) = u_0 e^{-2(s(x-1/2))^2}$. On the interval, the decay of $u(x, 0)$ is suffciently fast that we can consider the initial condition to be periodic. We set $n = 15$, $J = 4$, $\Delta t = 0.001$, and $\varepsilon = 10^{-6}$. For easy comparison with the results of [39], we choose $\nu = 0.0005$. The approximation to the solution of

$$u_t + uu_x - \nu u = \nu u_{xx}, \quad 0 \le x \le 1, t \ge 0, \tag{5.27}$$

is computed via

$$\begin{aligned} U(t_{i+1}) &= e^{\Delta t/(\nu-\Delta_x^2+I)} U(t_i) \\ &\quad - \tfrac{1}{2}\tilde{\Omega}_{\nu-\Delta_x^2,I}[U(t_i)-\partial_x U(t_{i+1}) + U(t_{i+1})-\partial_x U(t_i)], \end{aligned} \tag{5.28}$$

where

$$\tilde{\Omega}_{\nu-\Delta_x^2,I} = \frac{e^{\Delta t(\nu-\Delta_x^2+I)} - I}{\nu-\Delta_x^2 + I}, \tag{5.29}$$

and $I$ is the identity operator. We have chosen to use the operator $L$ in the form $L = \nu-\Delta_x^2 + I$ (see the development in, e.g., Section 2). We note that the NS-forms of the operators $e^{\Delta t(\nu-\Delta_x^2+I)}$

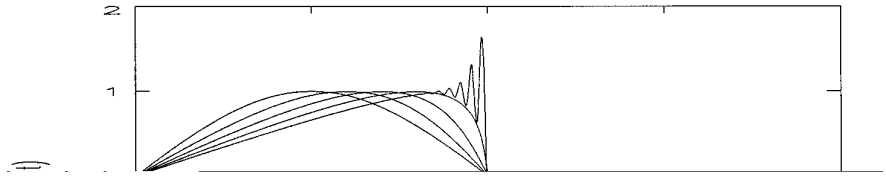


**FIG. 9.** The projection on $\mathbf{V}_0$ of the solution of Burgers' equation at various time steps computed via the iteration (5.21). In this experiment $n = 10$, $J = 4$, $Dt = 0.001$, $n = 0.001$, and $\varepsilon = 10^{-6}$. An analogue of the Gibbs phenomenon begins because the shock cannot be accurately represented by $n = 5$

**FIG. 11.** The projection on $\mathbf{V}_0$ of the solution of Burgers' equation at various time steps computed via the iteration (5.21). In this experiment $n = 15$, $J = 9$, $n = 5$

**FIG. 13.** The projection on $\mathbf{V}_0$


**FIG. 15.** The projection on $\mathbf{V}_0$ of the solution of (5.27) at various time steps. In this experiment $n = 15$, $J = 4$, $Dt = 0.001$, $\varepsilon = 10^{-6}$, and $n = 0.005$. This figure corresponds to Example 4 of the text.

(3.1) and (3.2), we note that the scaling function and wavelet are related by the two-scale difference equations

$$w(x) = \sqrt{2}$$

The function $c(?)$ has $M$ vanishing moments, i.e.,

$$\int_{-\infty}^{\infty} c(x)x^m\,dx = 0, \quad 0 \le m \le M-1, \qquad \text{(A.3)}$$

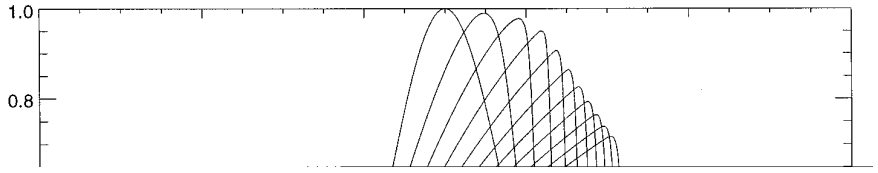


**FIG. 17.** The projection on $\mathbf{V}_0$ of the solution of cubic Burgers' equation (5.30) at various time steps, computed using a gaussian initial condition. In this experiment $n = 13$, $J = 6$, $Dt = 0.001$, $n = 0.001$, and $\varepsilon = 10^{-6}$. This figure corresponds to Example 5 of the text.

Let $P_j$ denote the projection operator onto subspace $\mathbf{V}_j$ and let $Q_j = P_{j-1} - P_j$ be the projection operator onto subspace $\mathbf{W}_j$. The projection of a function $f(x)$ onto subspace $\mathbf{V}_j$ is given by

$$(P_j f)(x) = \sum_{k \in Z} s_k^j w_{j,k}(x). \tag{A.6}$$

Alternatively, it follows from (3.2) and (A.6) that we can also write $(P_j f)(x)$ as a sum of projections of $f(x)$ onto subspaces $\mathbf{W}_{j'}$, $j' < j$,

$$(P_j f)(x) = \sum_{j' < j} \sum_{k \in Z} d_k^{j'} c_{j'}$$

The set of coefficients $\{s_k^j\}_{k \in Z}$, which we refer to as "averages," is computed via the inner product

$$s_k^j = \int_{-\infty}^{\infty} f(x) w_{j,k}(x)\, dx, \tag{A.8}$$

and the set of coefficients $\{d_k^j\}_{k \in Z}$, which we refer to as "differences," is computed via the inner product

$$d_k^j = \int_{-\infty}^{\infty} f(x) c_{j,k}(x)\, dx. \tag{A.9}$$

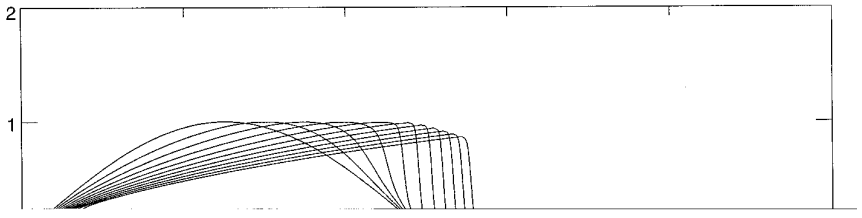


**FIG. 19.** The projection on $\mathbf{V}_0$ of the solution of cubic Burgers' equation (5.30) at various time steps, computed using a sinusoidal initial condition. In this experiment $n = 13$, $J = 6$, $Dt = 0.001$, $\nu = 0.001$, and $\varepsilon = 10^{-6}$. This figure corresponds to Example 5 of the text.

of a function $f(x)$ on $\mathbf{V}_0$ is given by a sum of successive projections on subspaces $\mathbf{W}_j$, $j = 1, 2, \ldots, J$, and a final "coarse" scale projection on $\mathbf{V}_J$,

$$(P_0 f)(x) = \sum_{j=1}^{J} \sum_{k \in \mathbb{F}_{2^{n-j}}} d_k^j$$

$$s_k^j = \sum_{l=1}^{L-1} h_l s_{l+2k-1}^{j-1}, \tag{A.11}$$

$$d_k^j = \sum_{l=1}^{L-1} g_l s_{l+2k-1}^{j-1}, \tag{A.12}$$

let representation of an operator in the NS-form is found by using bases formed by combinations of wavelet and scaling functions, for example, in $\mathbf{L}^2(\mathrm{R}^2)$,

$$c_{j,k}(x)\ c_{j,k9}(y$$

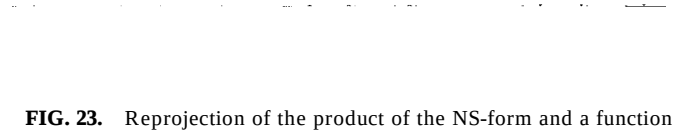

**FIG. 23.** Reprojection of the product of the NS-form and a function into a wavelet basis.

scale $j = 2, 3, \ldots, J-1$, we decompose $\|s^j\| = \|\hat{s}^j\| + \|\tilde{s}^j\|$ into $\|\tilde{s}^{j+1}\|$ and $\|\tilde{d}^{j+1}\|$ and form the sums $\|s^{j+1}\| = \|\hat{s}^{j+1}\| + \|\tilde{s}^{j+1}\|$ and $\|d^{j+1}\| = \|\hat{d}^{j+1}\| + \|\tilde{d}^{j+1}\|$. The sets $\|s^J\|$ and $\|d^j\|_{j=1}^{J}$ are the coefficients of the wavelet expansion of $(T_0 f_0)(x)$, i.e., the coefficients appearing in (A.17). This procedure is illustrated in Fig. 23.

$$\begin{aligned} a_l^j &= 2^{2pj} a_l^0, \\ b_l^j &= 2^{2pj} b_l^0, \\ c_l^j &= 2^{2pj} c_l^0, \\ s_l^j &= 2^{2pj} s_l^0, \end{aligned} \tag{A.19}$$

We note that if we were to use any other finite-difference representation as coefficients on $\mathbf{V}_0$, the coefficients on $\mathbf{V}_j$ would not be related by scaling and would require individual calculations for each $j$.

Using the two-scale difference equations (A.1) and (A.2), we are led to

$$a_l^j = 2 \sum_{k=0}^{L-1} \sum_{k \neq 0}^{L-1} g_k$$

A.3. *Proofs of Vanishing Moments Property*

*Proof of Lemma* 1. Using the definition (A.14), we obtain

$$\sum_{l=-\infty}^{\infty} l^m b_l = \int_{-\infty}^{\infty} c(x-k) f(-x) P_m(x)\, dx. \qquad \text{(A.25)}$$

We have used the fact that if the wavelet basis has $M$ vanishing moments, then

$$\sum_{l=-\infty}^{\infty} l^m w(x-l) = P_m(x), \qquad \text{(A.26)}$$

where $P_m(x)$ is a polynomial of degree $m$ for $0 \le m \le M-1$; see [31].

Since the function $f(?$

$$(Hg)(j) = -i\,\mathrm{sign}(j)\hat{g}(j), \qquad \text{(A.31)}$$

may be viewed as a generalized function, derivatives of which act on test functions $f \in C_0^\infty(\mathrm{R})$ as

$$\left[\frac{d^m}{dj^m}(-i\,\mathrm{sign}(j)\hat{g}(j)), f\right] = -i \sum_{j=1}^{m} \binom{m}{l} f^{(j-1)}(0)\hat{g}^{(m-j)}(0) - i\int_{-\infty}^{\infty} \mathrm{sign}(j)\hat{g}^{(m)}(j) f(j)\, dj. \qquad \text{(A.32)}$$

In order to show that $(Hc)(x)$ has $M$ vanishing moments, we recall that in the Fourier domain vanishing moments are characterized by

where $z = z(x, j, l)$ lies between $x$ and $x + 2^j l$, we compute $\overline{d}^j_k = \sum_l b^j_{k,l}$ which again is of the same order as $d^{j+1}_{k'}$. Therefore, if $\|d^{j+1}_{k'}\| \le \varepsilon$ for $k' \in \Gamma_{2^{J_2-(j+1)}}$, then for some constant $C$,

for $m = 1, 2, \ldots, M$ and arrive at

9. J. Bebernes and A. Lacey, Finite-time blowup for a particular parabolic system, *SIAM J. Math. Anal.* **21,** 1415 (1990).

32. Y. Meyer, *Le Calcul Scientifique, les Ondelettes et les Filtres Miroirs en Quadrature,* Centre de Recherche de Mathématiques de la Décision Report 9007.
33. M. V. Wickerhauser, *Adapted Wavelet Analysis from Theory to Software* (Peters, Wellesley, MA, 1994).
38. L. Gagnon and J. M. Lina, Wavelets and numerical split-step method: A global adaptive scheme, *Opt. Soc. Am. B,* to appear.
39. P. L. Sachdev, *Nonlinear Diffusive Waves* (Cambridge Univ. Press, Cambridge, 1987).
40. G. Beylkin, On the fast algorithm for multiplication of functions